in dodecane-dilute nitric acid. J. Inorg. Nucl. Chem. 1977, 39, 1425-1430.
Yoshizuka, K.; Kondo, K.; Nakashio, F. Extraction equilibria of Cu(II), Zn(II) and Co(II) with N-8-quinolylsulfonamide. J. Chem. Eng. Jpn. 1985, 18, 383-384.
Yoshizuka, K.; Kondo, K.; Nakashio, F. Effect of hydrophobicity on distribution and interfacial adsorption equilibria of N-8-quinolylsulfonamide. J. Chem. Eng. Jpn. 1986a, 19, 258-262.
Yoshizuka, K.; Kondo, K.; Nakashio, F. Effect of interfacial reaction on rates of extraction and stripping in membrane extractor using a hollow fiber. J. Chem. Eng. Jpn. 1986b, 19, 312-318.
Yoshizuka, K.; Kondo, K.; Nakashio, F. Effect of hydrophobicity of extractant on extraction kinetics of copper with N-8-quinolylsulfonamide. J. Chem. Eng. Jpn. 1986c, 19, 396-400.

*Received for review* June 12, 1991
*Revised manuscript received* January 21, 1992
*Accepted* February 20, 1992

# *PVT* Calculations on Petroleum Reservoir Fluids Using Measured and Estimated Compositional Data for the Plus Fraction

**Karen Schou Pedersen***
*CALSEP A/S, Lyngby Hovedgade 29, DK-2800 Lyngby, Denmark*

**Ann Lisbeth Blilie and Knut Kristian Meisingset**
*STATOIL, Forus, N-4001 Stavanger, Norway*

Molar compositions to $C_{80+}$ are presented for 17 North Sea oil mixtures. These extensive analytical data have been made available using a high-temperature gas chromatography technique. It is shown that a simple exponential distribution fits the $C_{7+}$ distribution of all 17 oil mixtures very well. Because of this simple exponential relation, it is possible from a compositional analysis (to for example $C_{10+}$ or $C_{20+}$) to generate an extended composition that can be used to perform accurate *PVT* and phase equilibrium calculations. There appears to be little or no advantage of having measured compositional analyses beyond $C_{20+}$.

## Introduction

The compositions of petroleum reservoir fluids are most often reported to $C_{7+}$, $C_{10+}$, or $C_{20+}$ and in rare cases to $C_{30+}$ (Pedersen et al., 1989a). To be able to perform phase equilibrium calculations (*PVT* calculations) on this kind of mixtures, it is necessary to estimate the molar composition of the plus fraction. The final calculation results are very sensitive to the molar distribution assumed for the plus fraction. Pedersen et al. (1985, 1989b) have obtained accurate *PVT* calculation results by using the Soave-Redlich-Kwong (SRK) equation of state (Soave, 1972) and assuming the following dependence of the mole fraction on carbon number:

$$z_n = \exp(A + BC_n) \quad (1)$$

$z_n$ is the total mole fraction of components with $C_n$ carbon atoms and $A$ and $B$ are constants. It has previously been shown (Pedersen et al., 1984) that this distribution function may be used to represent reservoir fluid compositions to at least $C_{19}$.

With the use of a high-temperature gas chromatography technique, analytical data have now been made available to $C_{80+}$ for 17 North Sea oil mixtures. These data have made it possible to check the validity of the distribution function expressed in eq 1, and to investigate whether the *PVT*-calculation accuracy can be improved by using analytical data to $C_{80+}$ as compared to the use of a distribution function for the $C_{10+}$, $C_{20+}$, or $C_{30+}$ fraction.

## Experimental Data

This paper deals with 17 different reservoir fluids (gas condensates and oils). The molar compositions of the reservoir fluids are determined from compositional analyses of the gas and liquid phases resulting from a flash of the reservoir fluid to atmospheric conditions or of the well test separator gas and liquid phases. In the latter case the separator liquid is flashed to standard conditions before the analysis is performed. The molar composition to $C_{10}$ of all samples was determined by capillary gas chromatography. For the liquid samples at atmospheric conditions (in the following referred to as oils or stable oils) the $C_{10+}$ composition to $C_{20+}$ or to $C_{30+}$ is usually determined by TBP distillation (Osjord et al., 1985). The resulting molar compositions are given in terms of carbon number fractions, as described by Katz and Firoozabadi (1978). A carbon number fraction, $C_n$, consists of all components with boiling points higher than that of the $n$-alkane with $n-1$ carbon atoms and lower than or equal to that of the $n$-alkane with $n$ carbon atoms. Molecular weights are calculated from the single-component distribution for the $C_6$-$C_9$ fractions and measured for the distillate fractions. Molar compositions determined in the described manner are in the following referred to as standard molar compositions. In Table I is shown at what plus fraction the standard molar composition stops for the oil referred to in the *PVT* calculations.

**Table I. Plus Fractions of the Standard Molar Compositions for 15 of the Reservoir Fluids of This Study**

| oil no. | plus fraction | oil no. | plus fraction | oil no. | plus fraction |
|---|---|---|---|---|---|
| 1 | $C_{10+}$ | 6 | $C_{10+}$ | 11 | $C_{10+}$ |
| 2 | $C_{30+}$ | 7 | $C_{20+}$ | 12 | $C_{20+}$ |
| 3 | $C_{20+}$ | 8 | $C_{20+}$ | 13 | $C_{17+}$ |
| 4 | $C_{10+}$ | 9 | $C_{20+}$ | 16 | $C_{10+}$ |
| 5 | $C_{20+}$ | 10 | $C_{20+}$ | 17 | $C_{20+}$ |

The extended molar compositions to $C_{80+}$ presented in this paper have been obtained using high-temperature capillary gas chromatography (GC) to analyze the stable oils (this technique is of no interest for gas phases because the content of $C_{10+}$ components is negligible). The applied technique is similar to that used by Curvers et al. (1989). The residue which does not pass through the high-tem-

0888-5885/92/2631-1378$03.00/0 

**Table II. Extended Molar Composition of Oil 1**

| compd | mole fraction | MW | $\rho$(15 °C, 1 atm), g/cm$^3$ |
|---|---|---|---|
| $C_1$ | 0.0013 | 16.0 | |
| $C_2$ | 0.0050 | 30.1 | |
| $C_3$ | 0.0047 | 44.1 | |
| $i$-$C_4$ | 0.0055 | 58.1 | |
| $C_4$ | 0.0062 | 58.1 | |
| $i$-$C_5$ | 0.0108 | 72.1 | |
| $C_5$ | 0.0050 | 72.1 | |
| $C_6$ | 0.0189 | 86.2 | |
| $C_7$ | 0.0534 | 90.9 | 0.749 |
| $C_8$ | 0.0854 | 105.0 | 0.768 |
| $C_9$ | 0.0704 | 117.7 | 0.793 |
| $C_{10}$ | 0.0680 | 132.0 | 0.808 |
| $C_{11}$ | 0.0551 | 148.0 | 0.815 |
| $C_{12}$ | 0.0500 | 159.0 | 0.836 |
| $C_{13}$ | 0.0558 | 172.0 | 0.850 |
| $C_{14}$ | 0.0508 | 185.0 | 0.861 |
| $C_{15}$ | 0.0466 | 197.0 | 0.873 |
| $C_{16}$ | 0.0380 | 209.0 | 0.882 |
| $C_{17}$ | 0.0267 | 227.0 | 0.873 |
| $C_{18}$ | 0.0249 | 243.0 | 0.875 |
| $C_{19}$ | 0.0214 | 254.0 | 0.885 |
| $C_{20}$ | 0.0223 | 262.0 | 0.903 |
| $C_{21}$ | 0.0171 | 281.0 | 0.898 |
| $C_{22}$ | 0.0142 | 293.0 | 0.898 |
| $C_{23}$ | 0.0163 | 307.0 | 0.899 |
| $C_{24}$ | 0.0150 | 320.0 | 0.900 |
| $C_{25}$ | 0.0125 | 333.0 | 0.905 |
| $C_{26}$ | 0.0145 | 346.0 | 0.907 |
| $C_{27}$ | 0.0133 | 361.0 | 0.911 |
| $C_{28}$ | 0.0123 | 374.0 | 0.915 |
| $C_{29}$ | 0.0115 | 381.0 | 0.920 |
| $C_{30}$ | 0.0109 | +624.0 | +0.953 |
| $C_{31}$ | 0.0090 | | |
| $C_{32}$ | 0.0092 | | |
| $C_{33}$ | 0.0079 | | |
| $C_{34}$ | 0.0067 | | |
| $C_{35}$ | 0.0070 | | |
| $C_{36}$ | 0.0059 | | |
| $C_{37}$ | 0.0049 | | |
| $C_{38}$ | 0.0052 | | |
| $C_{39}$ | 0.0046 | | |
| $C_{40}$ | 0.0037 | | |
| $C_{41}$–$C_{45}$ | 0.0159 | | |
| $C_{46}$–$C_{50}$ | 0.0106 | | |
| $C_{51}$–$C_{55}$ | 0.0074 | | |
| $C_{56}$–$C_{60}$ | 0.0056 | | |
| $C_{61}$–$C_{65}$ | 0.0041 | | |
| $C_{66}$–$C_{70}$ | 0.0033 | | |
| $C_{71}$–$C_{75}$ | 0.0027 | | |
| $C_{76}$–$C_{80}$ | 0.0025 | | |
| $C_{80+}$ | 0.0029 | | |

perature GC column was not quantified and therefore was neglected. This residue usually amounts to 1–10 wt % of the total $C_{30+}$ fraction.

In Tables II and III are shown the extended molar compositions of oils 1 and 2. Standard molar compositions of the reservoir fluids corresponding to oils 1 and 2 are shown in Tables IV and V. They are determined by combining oil and gas-phase compositions as described above. Extended molar compositions for the 15 remaining oils are contained in the supplementary material (see paragraph at end of paper regarding supplementary material).

*PVT* calculation results based on extended molar compositions to $C_{80+}$ have been compared with those of using a standard molar composition to $C_{10+}$, $C_{17+}$, $C_{20+}$, or $C_{30+}$ with the constants $A$ and $B$ in eq 1 determined from the mole fraction and molecular weight of the plus fraction. In this comparative study the following kinds of *PVT* data have been used: saturation point pressures (dew and bubble points); oil densities in differential depletion studies; gas-phase compressibility factors; separator gas/oil ratios. The employed *PVT* data are presented in the section *PVT* Calculations.

**Table III. Extended Molar Composition of Oil 2**

| compd | mole fraction | MW | $\rho$(15 °C, 1 atm), g/cm$^3$ |
|---|---|---|---|
| $C_2$ | 0.0001 | 30.1 | |
| $C_3$ | 0.0047 | 44.1 | |
| $i$-$C_4$ | 0.0058 | 58.1 | |
| $C_4$ | 0.0151 | 58.1 | |
| $i$-$C_5$ | 0.168 | 72.1 | |
| $C_5$ | 0.0196 | 72.1 | |
| $C_6$ | 0.0437 | 86.2 | |
| $C_7$ | 0.0900 | 92.3 | 0.734 |
| $C_8$ | 0.1071 | 105.9 | 0.756 |
| $C_9$ | 0.0732 | 120.3 | 0.775 |
| $C_{10}$ | 0.0623 | 133.0 | 0.789 |
| $C_{11}$ | 0.0550 | 148.0 | 0.794 |
| $C_{12}$ | 0.0514 | 163.0 | 0.806 |
| $C_{13}$ | 0.0443 | 177.0 | 0.819 |
| $C_{14}$ | 0.0480 | 190.0 | 0.832 |
| $C_{15}$ | 0.0381 | 204.0 | 0.834 |
| $C_{16}$ | 0.0282 | 217.0 | 0.844 |
| $C_{17}$ | 0.0333 | 235.0 | 0.841 |
| $C_{18}$ | 0.0234 | 248.0 | 0.847 |
| $C_{19}$ | 0.0266 | 260.0 | 0.860 |
| $C_{20}$ | 0.04177 | 269.0 | 0.874 |
| $C_{21}$ | 0.0171 | 283.0 | 0.870 |
| $C_{22}$ | 0.0148 | 298.0 | 0.872 |
| $C_{23}$ | 0.0156 | 310.0 | 0.875 |
| $C_{24}$ | 0.0113 | 322.0 | 0.877 |
| $C_{25}$ | 0.0112 | 332.0 | 0.881 |
| $C_{26}$ | 0.0097 | 351.0 | 0.886 |
| $C_{27}$ | 0.0110 | 371.0 | 0.888 |
| $C_{28}$ | 0.0073 | 382.0 | 0.895 |
| $C_{29}$ | 0.0088 | 394.0 | 0.898 |
| $C_{30}$ | 0.0065 | +612.0 | +0.935 |
| $C_{31}$ | 0.0060 | | |
| $C_{32}$ | 0.0062 | | |
| $C_{33}$ | 0.0054 | | |
| $C_{34}$ | 0.0045 | | |
| $C_{35}$ | 0.0046 | | |
| $C_{36}$ | 0.0038 | | |
| $C_{37}$ | 0.0033 | | |
| $C_{38}$ | 0.0034 | | |
| $C_{39}$ | 0.0035 | | |
| $C_{40}$ | 0.0021 | | |
| $C_{41}$–$C_{45}$ | 0.0099 | | |
| $C_{46}$–$C_{50}$ | 0.0064 | | |
| $C_{51}$–$C_{55}$ | 0.0045 | | |
| $C_{56}$–$C_{60}$ | 0.0031 | | |
| $C_{61}$–$C_{65}$ | 0.0023 | | |
| $C_{66}$–$C_{70}$ | 0.0018 | | |
| $C_{71}$–$C_{75}$ | 0.0014 | | |
| $C_{76}$–$C_{80}$ | 0.0012 | | |
| $C_{80+}$ | 0.0012 | | |

**Table IV. Standard Molar Composition of Reservoir Fluid 1**

| compd | mole fraction | MW | $\rho$(15 °C, 1 atm), g/cm$^3$ |
|---|---|---|---|
| $N_2$ | 0.004 03 | | |
| $CO_2$ | 0.010 00 | | |
| $C_1$ | 0.453 96 | | |
| $C_2$ | 0.042 02 | | |
| $C_3$ | 0.008 87 | | |
| $i$-$C_4$ | 0.005 61 | | |
| $C_4$ | 0.005 18 | | |
| $i$-$C_5$ | 0.006 47 | | |
| $C_5$ | 0.002 94 | | |
| $C_6$ | 0.010 11 | | |
| $C_7$ | 0.028 78 | 91.7 | 0.742 |
| $C_8$ | 0.041 14 | 105.0 | 0.768 |
| $C_9$ | 0.033 22 | 117.6 | 0.794 |
| $C_{10+}$ | 0.347 67 | 293.6 | 0.902 |

## Evaluation of Distribution Function

To test the ability of the distribution function shown

**Table V. Standard Molar Composition of Reservoir Fluid 2**

| compd | mole fraction | MW | $\rho$(15 °C, 1 atm), g/cm$^3$ |
|---|---|---|---|
| $N_2$ | 0.006 90 | | |
| $CO_2$ | 0.001 20 | | |
| $C_1$ | 0.470 60 | | |
| $C_2$ | 0.056 90 | | |
| $C_3$ | 0.043 90 | | |
| $i$-$C_4$ | 0.009 50 | | |
| $C_4$ | 0.024 20 | | |
| $i$-$C_5$ | 0.011 10 | | |
| $C_5$ | 0.014 60 | | |
| $C_6$ | 0.022 60 | | |
| $C_7$ | 0.039 30 | 91.9 | 0.735 |
| $C_8$ | 0.045 20 | 105.2 | 0.745 |
| $C_9$ | 0.032 30 | 121.0 | 0.784 |
| $C_{10}$ | 0.023 00 | 133.0 | 0.789 |
| $C_{11}$ | 0.020 30 | 148.0 | 0.794 |
| $C_{12}$ | 0.018 80 | 163.0 | 0.806 |
| $C_{13}$ | 0.016 20 | 177.0 | 0.819 |
| $C_{14}$ | 0.017 60 | 190.0 | 0.832 |
| $C_{15}$ | 0.013 90 | 204.0 | 0.834 |
| $C_{16}$ | 0.010 30 | 217.0 | 0.844 |
| $C_{17}$ | 0.012 20 | 235.0 | 0.841 |
| $C_{18}$ | 0.008 50 | 248.0 | 0.847 |
| $C_{19}$ | 0.009 70 | 260.0 | 0.860 |
| $C_{20}$ | 0.003 20 | 269.4 | 0.874 |
| $C_{21}$ | 0.008 00 | 282.5 | 0.870 |
| $C_{22}$ | 0.005 30 | 297.7 | 0.872 |
| $C_{23}$ | 0.004 40 | 310.1 | 0.875 |
| $C_{24}$ | 0.003 40 | 321.8 | 0.877 |
| $C_{25}$ | 0.004 80 | 332.4 | 0.881 |
| $C_{26}$ | 0.003 90 | 351.1 | 0.886 |
| $C_{27}$ | 0.003 10 | 370.8 | 0.888 |
| $C_{28}$ | 0.003 0 | 381.6 | 0.895 |
| $C_{29}$ | 0.002 40 | 393.7 | 0.898 |
| $C_{30+}$ | 0.029 40 | 612.0 | 0.935 |

**Table VI. Coefficient of Determination ($r^2$) Calculated Assuming the Distribution Function Expressed in Eq 1 for the Composition of 17 Different Oil Mixtures**

| oil no. | $r^2$ | oil no. | $r^2$ | oil no. | $r^2$ |
|---|---|---|---|---|---|
| 1 | 0.9873 | 7 | 0.9878 | 13 | 0.9432 |
| 2 | 0.9863 | 8 | 0.9842 | 14 | 0.9852 |
| 3 | 0.9852 | 9 | 0.9884 | 15 | 0.9865 |
| 4 | 0.9818 | 10 | 0.9924 | 16 | 0.9854 |
| 5 | 0.9764 | 11 | 0.9443 | 17 | 0.9894 |
| 6 | 0.9866 | 12 | 0.9949 | av | 0.9815 |

in eq 1 to represent the molar distributions of the $C_{7+}$ fractions of the 17 oils, the coefficient of determination, $r^2$

$$r^2 = \frac{[\sum x_i \ln y_i - (1/n)\ \sum x_i \sum \ln y_i]^2}{\left[\sum x_i^2 - \frac{(\sum x_i)^2}{n}\right]\left[\sum (\ln y_i)^2 - \frac{(\sum \ln y_i)^2}{n}\right]} \quad (2)$$

has been calculated for each mixture. In eq 2 $x_i$ and $y_i$ are paired values of observations and $n$ is the number of observations. Assuming the distribution function of eq 1, $x_i$ and $y_i$ are corresponding values of carbon number and mole fraction. The value of $r^2$ will lie between 0 and 1 and will indicate how closely the equation considered fits the experimental data. The closer $r^2$ is to 1, the better the fit.

The final values for $r^2$ for each of the 17 oil mixtures are shown in Table VI. The average value of $r^2$ obtained using the distribution function of eq 1 is 0.9815. It is very close to 1, and it can therefore be concluded that eq 1 represents the experimental molar distributions very closely.

In Figures 1–4 are shown experimental and calculated results for the mole fraction versus carbon number for oils 1–4. The squares are experimental values for single carbon number fractions, while the crosses are based on data for groups of five fractions ($C_{41-45}$, $C_{46-50}$, etc.). The solid line represents the best fit from $C_7$ to $C_{80}$ according to eq 1.

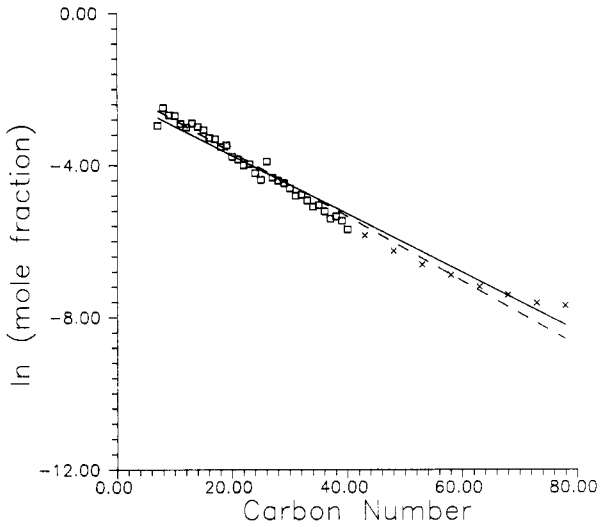


**Figure 1.** Experimental (□ and ×) and calculated molar distributions of oil 1. The solid line is based on compositional data to $C_{80+}$, and the dashed line is based on compositional data to $C_{10+}$.

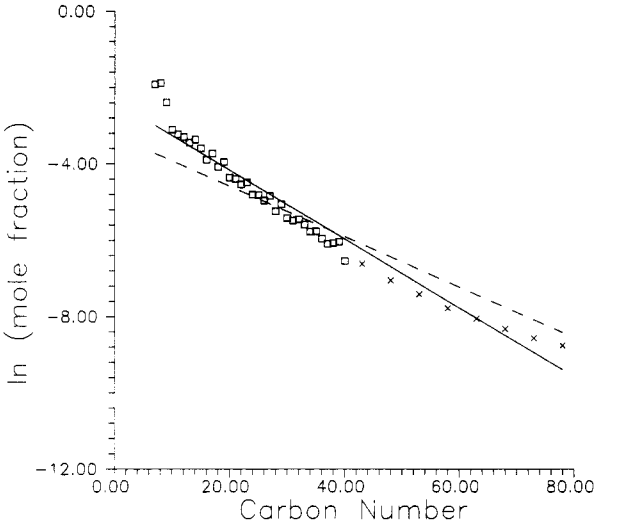


**Figure 2.** Experimental (□ and ×) and calculated molar distributions of oil 2. The solid line is based on compositional data to $C_{80+}$, and the dashed line is based on compositional data to $C_{30+}$.

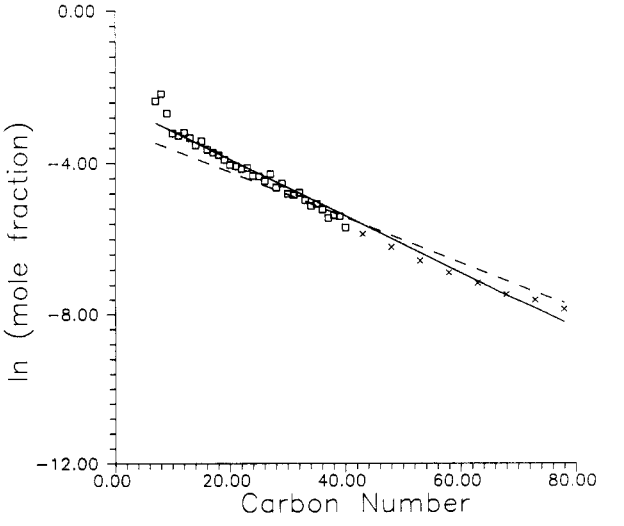


**Figure 3.** Experimental (□ and ×) and calculated molar distributions of oil 3. The solid line is based on compositional data to $C_{80+}$, and the dashed line is based on compositional data to $C_{20+}$.

Table VII. Values of the Coefficients Entering into Eqs 3–5

| coeff | value | coeff | value |
|---|---|---|---|
| $c_1$ | $1.6312 \times 10^2$ | $d_3$ | $2.0846 \times 10^{-2}$ |
| $c_2$ | $8.6052 \times 10$ | $d_4$ | $-3.9872 \times 10^3$ |
| $c_3$ | $4.3475 \times 10^{-1}$ | $e_1$ | $7.4310 \times 10^{-1}$ |
| $c_4$ | $-1.8774 \times 10^3$ | $e_2$ | $4.8122 \times 10^{-3}$ |
| $d_1$ | $-1.3408 \times 10^{-1}$ | $e_3$ | $9.6707 \times 10^{-3}$ |
| $d_2$ | 2.5019 | $e_4$ | $-3.7184 \times 10^{-6}$ |

The dashed line represents the distribution function determined by eq 1 using only the standard molar composition and the plus-fraction molecular weight.

The $A$ and $B$ parameters are determined from the mole fraction and the molecular weight of the plus fraction. It is assumed that the dependence of the molecular weight against carbon number can be described by the following equation:

$$\mathrm{MW} = 14C_n - 4 \tag{3}$$

## *PVT* Calculations

Various *PVT* properties have been measured for the 15 reservoir fluids of this study. Using the SRK equation in the modified form suggested by Peneloux et al. (1982), it has been investigated how closely the measured *PVT* properties can be predicted using standard molar compositions and using extended molar compositions. The critical temperatures and pressures and the acentric factors of the $C_{7+}$ fractions are calculated using the following relations (Pedersen et al., 1989b):

$$T_c = c_1\rho + c_2 \ln \mathrm{MW} + c_3\mathrm{MW} + c_4/\mathrm{MW} \tag{4}$$

$$P_c = d_1\rho + d_2\rho = d_3/\mathrm{MW} + d_4/\mathrm{MW}^2 \tag{5}$$

$$m = e_1\rho + e_2\mathrm{MW} + e_3\rho + e_4\mathrm{MW}^2 \tag{6}$$

where the values of the coefficients $c_1$–$c_4$, $d_1$–$d_4$, and $e_1$–$e_4$ are given in Table VII and $m$ is the following function of the acentric factor $\omega$:

$$m = 0.480 + 1.574\omega - 0.176\omega^2 \tag{7}$$

The densities entering into eqs 4–7 are estimated as described by Pedersen et al. (1984). The molecular weights are determined from eq 3. When the extended molar compositions are used, the $C_{41-45}$ fraction is attributed the molecular weight of $C_{43}$, the $C_{46-50}$ fraction is attributed the molecular weight of $C_{48}$, etc. The $C_{80+}$ fraction is attributed the molecular weight of $C_{90}$.

Binary interaction coefficients of zero are assumed for the hydrocarbon–hydrocarbon interactions while nonzero values are used for interactions with non-hydrocarbons (Pedersen et al., 1989a). The volume translation parameter entering into the Peneloux modification of the SRK equation has, for defined components ($N_2$, $CO_2$, $C_2$–$C_6$), been determined as suggested by Peneloux. For $C_{7+}$ components the volume translation parameter has been determined as the value which fits the measured density of that fraction at standard conditions. Before the *PVT* calculations are performed, some of the $C_{7+}$ fractions are grouped together. Twelve $C_{7+}$ fractions of approximately equal weight were used in the final calculations.

Two parallel series of *PVT* calculations have been performed with the purpose of investigating whether it is possible to improve the quality of the calculations by using extended compositional data instead of standard compositional data. In Table VIII are shown measured and calculated saturation pressures for each of the 15 reservoir fluids. Table IX shows results for experimental and calculated single-stage gas/oil ratios for 10 of the 15 reservoir fluids. Tables X and XI show experimental and calculated multistage separator gas/oil ratios for the reservoir fluids 1 and 7, respectively. In Tables XII and XIII are shown

Table VIII. Experimental and Calculated Saturation Point Pressures of the Reservoir Fluids[a]

| fluid no. | temp, °C | expt, bar | std comp, bar | % dev | ext comp, bar | % dev |
|---|---|---|---|---|---|---|
| 1 | 71.6 | 239.0 (b) | 237.4 | −0.7 | 224.7 | −6.0 |
| 2 | 72.8 | 237.0 (b) | 231.3 | −2.4 | 214.8 | −9.4 |
| 3 | 106.0 | 203.0 (b) | 394.9 | −2.0 | 381.7 | −5.3 |
| 4 | 150.5 | 631.0 (d) | 444.8 | −29.5 | 557.1 | −11.7 |
| 5 | 127.0 | 393.1 (b) | 382.5 | −2.7 | 376.6 | −4.2 |
| 6 | 125.0 | 404.8 (b) | 394.4 | −2.6 | 378.6 | −6.5 |
| 7 | 90.0 | 223.5 (b) | 211.5 | −5.4 | 208.5 | −6.7 |
| 8 | 77.0 | 101.0 (b) | 99.5 | −1.5 | 97.2 | −3.8 |
| 8 | 97.0 | 108.5 (b) | 107.2 | −1.2 | 106.6 | −1.8 |
| 9 | 117.0 | 114.0 (b) | 114.1 | 0.1 | 111.1 | −2.5 |
| 9 | 130.0 | 379.0 (b) | 386.4 | 2.0 | 383.7 | 1.2 |
| 10 | 112.0 | 244.5 (b) | 228.2 | −6.7 | 231.2 | −5.4 |
| 11 | 84.0 | 190.9 (b) | 215.0 | 13.2 | 182.5 | −3.9 |
| 12 | 129.0 | 477.0 (d) | 475.6 | −0.3 | 473.2 | −0.8 |
| 13 | 80.0 | 209.0 (d) | 181.4 | −13.2 | 205.9 | −1.5 |
| 16 | 100.0 | 61.5 (b) | 73.1 | 18.9 | 66.1 | 7.5 |
| 17 | 122.0 | 367.3 (b) | 364.6 | −0.7 | 375.9 | 2.3 |
| % ABS | | | | 6.1 | | 4.7 |
| % BIAS | | | | −2.0 | | −3.4 |

[a] (b), bubble point; (d), dew point. % dev = 100 × (calculated result − experimental result)/experimental result.

Table IX. Experimental and Calculated Single-Stage-Flash Gas/Oil Ratios (std m³ of Gas/std m³ of Oil)[a]

| fluid no. | temp, °C | press., bar | expt, m³/m³ | std comp, m³/m³ | % dev | ext comp, m³/m³ | % dev |
|---|---|---|---|---|---|---|---|
| 2 | 15.0 | 1.0 | 168.0 | 163.2 | −3.1 | 161.6 | −4.0 |
| 3 | 15.0 | 1.0 | 339.0 | 324.0 | −4.4 | 329.0 | −2.9 |
| 4 | 60.0 | 45.9 | 9900.0 | 10196.0 | 3.0 | 9982.0 | 0.8 |
| 6 | 15.0 | 1.0 | 210.0 | 210.0 | 0.0 | 208.9 | −0.5 |
| 7 | 15.0 | 1.0 | 148.2 | 150.6 | 1.6 | 151.2 | 2.0 |
| 9 | 15.0 | 1.0 | 188.6 | 181.3 | −3.9 | 181.1 | −4.0 |
| 11 | 23.0 | 1.0 | 51.6 | 51.4 | −0.4 | 50.3 | −2.5 |
| 12 | 36.0 | 52.0 | 898.0 | 867.2 | −3.4 | 867.9 | −3.4 |
| 13 | 32.0 | 60.7 | 18844.0 | 16833.0 | −10.7 | 16461.0 | −12.6 |
| 16 | 15.0 | 1.0 | 25.3 | 24.9 | −1.6 | 24.5 | −3.2 |
| % ABS | | | | | 3.2 | | 3.6 |
| % BIAS | | | | | −2.3 | | −3.0 |

[a] % dev is defined in Table VIII.

Table X. Experimental and Calculated Separator Gas/Oil Ratios of Reservoir Fluid No. 1 (std m³ of Gas/m³ of Separator Oil)

| temp, °C | press., bar | expt, m³/m³ | std comp, m³/m³ | % dev | ext comp, m³/m³ | % dev |
|---|---|---|---|---|---|---|
| 55.4 | 69.7 | 63.8 | 66.2 | 3.8 | 64.3 | 0.8 |
| 67.9 | 55.4 | 21.8 | 20.5 | −6.0 | 21.5 | −1.4 |
| 64.2 | 1.0 | 7.8 | 9.8 | 25.6 | 10.2 | 30.8 |
| % ABS | | | | 11.8 | | 11.0 |
| % BIAS | | | | 7.8 | | 10.0 |

[a] % dev is devined in Table VIII.

Table XI. Experimental and Calculated Separator Gas/Oil Ratios of Reservoir Fluid No. 7 (std m³ of Gas/m³ of Separator Oil)[a]

| temp, °C | press., bar | expt, m³/m³ | std comp, m³/m³ | % dev | ext comp, m³/m³ | % dev |
|---|---|---|---|---|---|---|
| 81.1 | 70.0 | 98.8 | 94.7 | −4.1 | 94.7 | −4.1 |
| 77.8 | 26.0 | 26.3 | 25.9 | −1.5 | 26.2 | −0.4 |
| 72.2 | 8.0 | 12.8 | 12.8 | 0.0 | 12.9 | 0.8 |
| 68.9 | 1.9 | 7.0 | 10.5 | 50.0 | 10.6 | 51.4 |
| % ABS | | | | 13.9 | | 14.2 |
| % BIAS | | | | 11.1 | | 11.9 |

[a] % dev is defined in Table VIII.

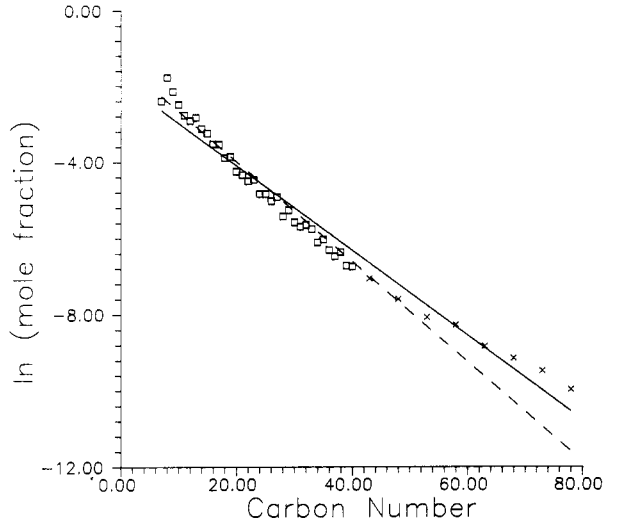


**Figure 4.** Experimental (□ and ×) and calculated molar distributions of oil 4. The solid line is based on compositional data to $C_{80+}$, and the dashed line is based on compositional data to $C_{10+}$.

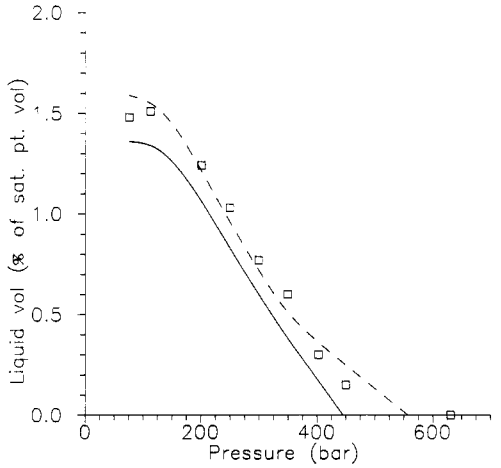


**Figure 5.** Measured (□) and calculated liquid dropout curves for mixture 4 at $T$ = 150.5 °C. The solid line shows calculation results based on standard compositional data and, the dashed line shows the results of using extended compositional data.

**Table XII. Experimental and Calculated Liquid Densities of Reservoir Fluid No. 1 at $T$ = 71.6 °C (Differential Liberation Data)[a]**

| press., bar | expt, g/cm³ | std comp, g/cm³ | % dev | ext comp, g/cm³ | % dev |
|---|---|---|---|---|---|
| 239.0 | 0.761 | 0.774 | 1.7 | 0.769 | 1.1 |
| 220.6 | 0.766 | 0.779 | 1.7 | 0.769 | 0.4 |
| 191.5 | 0.774 | 0.788 | 1.8 | 0.779 | 0.6 |
| 161.5 | 0.782 | 0.798 | 2.0 | 0.789 | 0.9 |
| 131.7 | 0.790 | 0.808 | 2.3 | 0.800 | 1.3 |
| 101.5 | 0.799 | 0.819 | 2.5 | 0.811 | 1.5 |
| 71.7 | 0.809 | 0.830 | 2.6 | 0.822 | 1.6 |
| 31.5 | 0.822 | 0.845 | 2.8 | 0.838 | 1.9 |
| % ABS | | | 2.2 | | 1.2 |
| % BIAS | | | 2.2 | | 1.2 |

[a] % dev is defined in Table VIII.

experimental and calculated liquid-phase densities of the reservoir fluids 1 and 3. The results are for differential liberation experiments. In Tables XIV and XV are shown measured and calculated gas-phase compressibility factors of the reservoir fluids 4 and 12 at rather high pressures.

Liquid dropout curves of mixtures 4, 12, and 13 are shown in Figures 5–7. The results for mixtures 4 and 12 are for constant mass expansion experiments while the results for mixture 13 are for a constant volume depletion experiment.

**Table XIII. Experimental and Calculated Liquid Densities of Reservoir Fluid No. 3 at $T$ = 106 °C (Differential Liberation Data)[a]**

| press., bar | expt, g/cm³ | std comp, g/cm³ | % dev | ext comp, g/cm³ | % dev |
|---|---|---|---|---|---|
| 352.4 | 0.619 | 0.629 | 1.6 | 0.616 | -0.5 |
| 302.8 | 0.642 | 0.653 | 1.7 | 0.642 | 0.0 |
| 246.0 | 0.666 | 0.679 | 2.0 | 0.669 | 0.5 |
| 176.7 | 0.693 | 0.710 | 2.5 | 0.702 | 1.3 |
| 101.7 | 0.724 | 0.746 | 3.0 | 0.740 | 2.2 |
| 30.2 | 0.758 | 0.786 | 3.7 | 0.781 | 3.0 |
| 3.9 | 0.791 | 0.813 | 2.8 | 0.809 | 2.3 |
| % ABS | | | 2.4 | | 1.4 |
| % BIAS | | | 2.4 | | 1.1 |

[a] % dev is defined in Table VIII.

**Table XIV. Experimental and Calculated Gas-Phase Compressibility Factors of Reservoir Fluid No. 4 at $T$ = 150.5 °C[a]**

| press., bar | expt | std comp | % dev | ext comp | % dev |
|---|---|---|---|---|---|
| 899.7 | 1.5421 | 1.5727 | 2.0 | 1.5734 | 2.0 |
| 852.7 | 1.4940 | 1.5268 | 2.2 | 1.5276 | 2.2 |
| 797.9 | 1.4331 | 1.4736 | 2.8 | 1.4743 | 2.9 |
| 754.3 | 1.3889 | 1.4314 | 3.1 | 1.4320 | 3.1 |
| 698.7 | 1.3315 | 1.3779 | 3.5 | 1.3785 | 3.5 |
| 651.1 | 1.2841 | 1.3325 | 3.8 | 1.3330 | 3.8 |
| 638.6 | 1.2706 | 1.3207 | 3.9 | 1.3212 | 4.0 |
| 631.0 | 1.2627 | 1.3135 | 4.0 | 1.3140 | 4.1 |
| % ABS | | | 3.2 | | 3.2 |
| % BIAS | | | 3.2 | | 3.2 |

[a] % dev is defined in Table VIII.

**Table XV. Experimental and Calculated Gas-Phase Compressibility Factors of Reservoir Fluid No. 12 at $T$ = 159 °C[a]**

| press., bar | expt | std comp | % dev | ext comp | % dev |
|---|---|---|---|---|---|
| 598.0 | 1.409 | 1.414 | 0.4 | 1.414 | 0.4 |
| 558.5 | 1.343 | 1.352 | 0.7 | 1.351 | 0.7 |
| 548.6 | 1.324 | 1.336 | 0.9 | 1.336 | 0.9 |
| 536.7 | 1.306 | 1.317 | 0.8 | 1.317 | 0.8 |
| 509.1 | 1.261 | 1.274 | 1.0 | 1.273 | 0.9 |
| 489.7 | 1.230 | 1.243 | 1.0 | 1.242 | 1.0 |
| 477.0 | 1.208 | 1.223 | 1.2 | 1.222 | 1.2 |
| % ABS | | | 0.9 | | 0.8 |
| % BIAS | | | 0.9 | | 0.8 |

[a] % dev is devined in Table VIII.

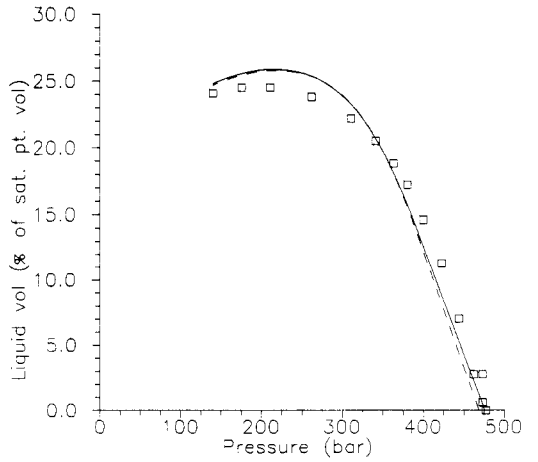


**Figure 6.** Measured (□) and calculated liquid dropout curves for mixture 12 at $T$ = 129 °C. The solid line shows calculation results based on standard compositional data, and the dashed line shows the results of using extended compositional data.

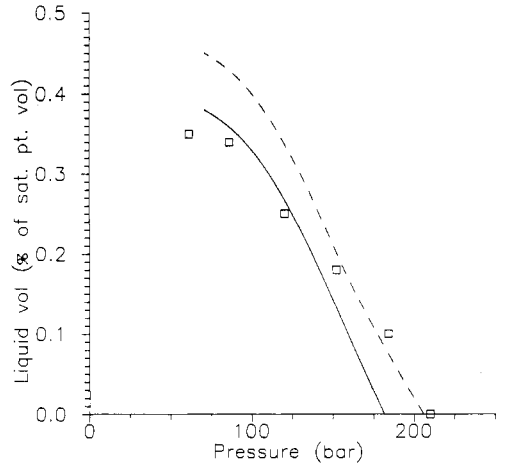


**Figure 7.** Measured (□) and calculated liquid dropout curves for mixture 13 at $T$ = 80 °C. The solid line shows calculation results based on standard compositional data, and the dashed line shows the results of using extended compositional data.

## Discussion of the Results

The parameter regression clearly indicates that the assumption of an exponential molar distribution against carbon number is reasonable. It must therefore be expected that it is possible to perform accurate *PVT* calculations using a less extensive compositional analysis than that provided using the high-temperature gas chromatography technique. In Figures 1–4 are shown molar distributions which are based on regressions to analytical data to $C_{80+}$ together with estimated distributions for $C_{10+}$, $C_{20+}$, or $C_{30+}$ fractions where the estimations are based on eq 1 and the $A$ and $B$ values determined from the mole fraction and the molecular weight of the plus fraction of the standard molar composition. For oils 1 and 3 the measured and the estimated molar distributions are in close agreement. For oils 2 and 4 there is some deviation. This deviation must be expected to be less important for mixture 2 than for mixture 4 because a standard molar composition to $C_{30+}$ is available for the latter mixture.

When the reservoir fluid saturation points calculated on the basis of standard molar compositions are compared with those calculated on the basis of extended molar compositions (Table VI), it is seen that the results obtained for fluids 4, 11, 13, and 16 using standard compositions are of a somewhat lower quality than the results obtained with extended molar compositions. For three of these mixtures (4, 11, and 16) the standard compositional data stop at $C_{10+}$. For the last one (mixture 13) the compositional data stop at $C_{17+}$ and no molecular weight is available for the $C_{17+}$ fraction. This indicates that an analysis must be available at least to $C_{20+}$ to achieve the best possible accuracy in the *PVT* calculations. For the remaining mixtures where a standard compositional analysis is available to $C_{20+}$ or to $C_{30+}$, the saturation point predictions based on standard molar compositions are generally better than those based on extended molar compositions. The reason for this is probably that the correlations used to calculate the equation of state parameters have been optimized against standard compositional data. The small errors which are introduced via the distribution function are accounted for by the choice of equation of state parameters. Another potential reason for the differences in calculation results could be that the $C_{80+}$ fraction is underestimated in the high-temperature GC results because the residue which does not pass through the column is neglected.

The results obtained for gas/oil ratios and phase densities using standard molar compositions are fairly close to those obtained using extended molar compositions. This was to be expected. Gas/oil ratios are not very sensitive to the details of the molar distribution assumed for the heavy end.

For mixtures 4 and 13 the calculation accuracy for the liquid dropout curves can be improved by using extended molar compositions instead of standard molar compositions. For mixture 12 there is almost no difference between the results obtained using standard and extended molar compositions. As already mentioned, the standard molar compositions for mixtures 4 and 13 stop at $C_{10+}$ while for mixture 12 a standard molar composition is available to $C_{20+}$. This is another indication that it is essential to have a molar composition to $C_{20+}$. Analytical data in addition to that do not markedly influence the calculation accuracy.

## Conclusion

With the use of experimental molar compositions to $C_{80+}$ for 17 different North Sea reservoir fluids, it has been shown that a simple exponential distribution function fits the plus fraction of reservoir fluids very well. By comparing *PVT* predictions based on compositional analyses to $C_{10+}$, to $C_{20+}$, and to $C_{80+}$, it is shown that compositional data are needed to $C_{20+}$ to accurately determine the parameters of the exponential distribution. There appears to be little or no advantage of having measured compositional analyses beyond $C_{20+}$.

## Nomenclature

$A$ = constant defined in eq 1
ABS = average absolute deviation
$B$ = constant defined in eq 1
BIAS = average deviation
$c_1$–$c_4$ = coefficients defined in eq 3 and in Table VII
$d_1$–$d_4$ = coefficients defined in eq 4 and in Table VII
$e_1$–$e_4$ = coefficients defined in eq 5 and in Table VII
$C_n$ = carbon number
MW = molecular weight
$m$ = function of the acentric factor defined in eq 6
$n$ = number of observations
$P_c$ = critical pressure
$r^2$ = correlation coefficient
TBP = true boiling point
$T_c$ = critical temperature
$x_i$ = $x$-value of $i$th observation
$y_i$ = $y$-value of $i$th observation
$z_n$ = total mole fraction of components with $C_n$ carbon atoms
% dev = percent deviation

*Greek Symbols*

$\omega$ = acentric factor
$\rho$ = density in g/cm$^3$ at 15 °C and 1 atm

**Supplementary Material Available:** Tables A1–A15 listing extended molar compositions of oils 3–17 (29 pages). Ordering information is given on any current masthead page.

## Literature Cited

Curvers, J.; van den Engel, P. Gas Chromatographic Method for Simulated Distillation up to a Boiling Point of 750 °C Using Temperature Programmed Injection and High Temperature Fused Silica Wide-Bore Columns. *J. High Resolut. Chromatogr.* **1989**, *12*, 16.

Katz, D. L.; and Firoozabadi, A. Predicting Phase Behavior of Condensate/crude Oil Systems Using Methane Interaction Coefficients. *J. Pet. Technol.* **1978**, *20*, 1649.

Osjord, E. H.; Rønningsen, H. P.; Tau, L. Distribution of Weight, Density and Molecular Weight in Crude Oil Derived from Computerized Capillary GC Analysis. *J. High Resolut. Chromatogr.*

*Chroamtogr. Commun.* **1985**, *8*, 684.
Pedersen, K.; Thomassen, P.; Fredenslund, Aa. Thermodynamics of Petroleum Mixtures Containing Heavy Hydrocarbons. 1. Phase Envelope Calculations by Use of the Soave-Redlich-Kwong Equation of State *Ind. Eng. Chem. Process Des. Dev.* **1984**, *23*, 163.
Pedersen, K. S.; Thomassen, P.; Fredenslund, Aa. Thermodynamics of Petroleum Mixtures Containing Heavy Hydrocarbons. 3. Efficient Flash Calculation Procedures Using the SRK Equation of State. *Ind. Eng. Chem. Process Des. Dev.* **1985**, *24*, 948.
Pedersen, K. S.; Fredenslund, Aa.; Thomassen, P. *Properties of Oils and Natural Gases*; Gulf: 1989a.
Pedersen, K. S.; Thomassen, P.; Fredenslund, Aa. Characterization of Gas Condensate Mixtures. *Adv. Thermodyn.* **1989b**, *1*, 137.
Peneloux, A.; Rauzy, E.; Freze, R. A Consistent Correction for Redlich-Kwong-Soave Volumes. *Fluid Phase Equilib.* **1982**, *8*, 7.
Soave, G. Equilibrium Constants from a Modified Redlich-Kwong Equation of State. *Chem. Eng. Sci.* **1972**, *27*, 1197.

*Received for review* July 17, 1991
*Revised manuscript received* November 11, 1991
*Accepted* February 19, 1992

# Local Heat Transfer in a Mixing Vessel Using Heat Flux Sensors

**Seungjoo Haam and Robert S. Brodkey***
*Department of Chemical Engineering, The Ohio State University, 140 West 19th Avenue, Columbus, Ohio 43210-1180*

**Julian B. Fasano**†
*Chemineer Inc., P.O. Box 1123, Dayton, Ohio 45401*

A rapid, computer based, local heat-transfer sensor system has been developed. The concept was to provide a quick, accurate, and efficient technique for the determination of process side heat-transfer coefficient models through the use of heat flux sensors and PC data acquisition. The system has been thoroughly tested. System noise and typical sensor variation with time have been studied; however, only part of the noise is real: the remainder is associated and correlatable with specific physical phenomena (vortical motions) that occur in the mixing vessel. A detailed study of the variation of the local coefficients as a function of angular position relative to the baffles is presented. The influence due to the presence of baffles can be seen and explained. Some typical results are given to illustrate the effect of the primary variable, Reynolds number. The relative level of effects from other design variables are presented.

## Introduction

Heat transfer in agitated vessels is a common operation in chemical processing. The rate of heat transfer during mixing of liquids depends on the type of the agitator, the design of the vessel, and processing conditions. In this research, the heat transfer at the wall of an agitated vessel with a dished bottom and four baffles was investigated. Three well-known impeller types were studied. The contents (water) of the vessel were slowly cooled by natural convection from the outer surface and small local cooling exchangers located directly under the sensors. The heat-transfer measurements were made by Micro-Foil heat flux sensors that are placed on the inside surface of the vessel. These sensors exhibit a potential directly proportional to the heat flux and are calibrated by the manufacturer. Thus, process side heat-transfer coefficients were determined. Determining heat-transfer coefficients by conventional thermocouple and heat balance technique is arduous and time consuming. The use of the thermophile style heat flux sensor to measure the heat flux and temperature of the wall would be a useful and a viable means of making point to point local measurements. For data acquisition, MetraByte's DAS-8 data acquisition system was used. Two BASIC programs were developed for data acquisition and determination of the heat-transfer coefficients and other important values. The goal of this research was to create a quick, accurate, and efficient system for the determination of process side local heat-transfer coefficients through the use of heat flux sensors and a PC based data acquisition system.

†Technical Director.

## Literature Review

Heat transfer in an agitated vessel is defined as

$$q = U_i A_i (T_o - T_i) \tag{1}$$

where $U_i$ = the overall heat-transfer coefficient, $A_i$ = the heat-transfer area, $T_o$ = temperature of the heat-transfer fluid, and $T_i$ = temperature of the process fluid.

If fouling factors are negligible, the overall heat-transfer coefficient can be described in terms of three separated heat-transfer resistances:

$$U_i = 1/[(1/h_i) + (\Delta r/k_w)(A_i/A_w) + (1/h_o)(A_i/A_0)] \tag{2}$$

See, for example, Chemineer Co. (1985), Chapman and Holland (1965a,b), and Poggeemann et al. (1980). In eq 2, the first term is the inside film coefficient, $h_i$, that is on the process liquid side of the surface. The second term is the conduction through the wall, and the third term is the outside film coefficient.

**Dimensional Analysis for Heat-Transfer Coefficient.** The inside or process side heat-transfer coefficient can be defined from the heat flow, $q$, heat-transfer area, $A_i$, and the temperature difference between the inside wall and the bulk of the fluid, $\Delta T_i$:

$$h_i = q/A_i(\Delta T_i) \tag{3}$$

The heat flow, $q$, can be determined from the temperature gradient at the inside wall of the vessel:

$$q = \int \int_s \left(k\left(\frac{dT}{dr}\right)_i\right) dS \tag{4}$$

0888-5885/92/2631-1384$03.00/0 